

SynGhost: Invisible and Universal Task-agnostic Backdoor Attack via Syntactic Transfer

Pengzhou Cheng¹, Wei Du¹, Zongru Wu¹, Fengwei Zhang², Libo Chen¹,
Zhuosheng Zhang^{1*}, Gongshen Liu¹

¹ School of Electronic Information and Electrical Engineering
Shanghai Jiao Tong University

² Department of Computer Science and Engineering
Southern University of Science and Technology
{cpztsm520, ddddw, wuzongru, bob777, zhangzs, lgshen}@sjtu.edu.cn
zhangfw@sustech.edu.cn

Abstract

Although pre-training achieves remarkable performance, it suffers from task-agnostic backdoor attacks due to vulnerabilities in data and training mechanisms. These attacks can transfer backdoors to various downstream tasks. In this paper, we introduce `maxEntropy`, an entropy-based poisoning filter that mitigates such risks. To overcome the limitations of manual target setting and explicit triggers, we propose SynGhost, an invisible and universal task-agnostic backdoor attack via syntactic transfer, further exposing vulnerabilities in pre-trained language models (PLMs). Specifically, SynGhost injects multiple syntactic backdoors into the pre-training space through corpus poisoning, while preserving the PLM’s pre-training capabilities. Second, SynGhost adaptively selects optimal targets based on contrastive learning, creating a uniform distribution in the pre-training space. To identify syntactic differences, we also introduce an awareness module to minimize interference between backdoors. Experiments show that SynGhost poses significant threats and can transfer to various downstream tasks. Furthermore, SynGhost resists defenses based on perplexity, fine-pruning, and `maxEntropy`. The code is available at <https://github.com/Zhou-CyberSecurity-AI/SynGhost>.

1 Introduction

Pre-training is a critical step for transformer-based language models, owing to the ability to learn generic knowledge in language modeling (Devlin et al., 2018). Given the substantial resources required for training, the online model hub efficiently hosts pre-trained language models (PLMs) (Cheng et al., 2023). Users can download and then

fine-tune PLMs on downstream tasks, or apply parameter-efficient fine-tuning (PEFT) to reduce computational cost (Wei et al., 2024). However, such supply chains are untrustworthy (Zhang et al., 2022). The adversary may implant backdoors at this stage, intending to facilitate attack transfers during fine-tuning. Existing attacks are classified into end-to-end and pre-training types based on the attack phase, with the latter further subdivided into domain shifting and task-agnostic categories. These attacks differ in their capabilities:

- **Effectiveness:** The adversary usually achieves high attack performance in end-to-end scenarios (Qiang et al., 2024; Zhao et al., 2024b), while the pre-trained backdoors primarily rely on explicit triggers (e.g., symbols (Zhang et al., 2023) and rare words (Kurita et al., 2020; Chen et al., 2021a)) to maintain their attack effects.

- **Stealthiness:** End-to-end attacks leverage various trigger design, such as syntax (Qi et al., 2021c), style (Qi et al., 2021b), sentences (Zhao et al., 2024a), and glyphs (Long et al., 2024) to improve stealth. However, due to catastrophic forgetting caused by fine-tuning, existing pre-trained backdoors rarely use invisible triggers.

- **Universality:** The former fails due to its close coupling with a specific task. Domain shifting backdoors relax this limitation but exhibit relatively weak influence when the domain gap is larger (Yang et al., 2021a). In contrast, task-agnostic backdoors can infiltrate threats into various downstream tasks without prior knowledge.

Thus, task-agnostic backdoors have a significant impact on PLMs. However, these attacks rely on explicit triggers (Shen et al., 2021; Chen et al., 2021a), which are easily detected by defenses. To demonstrate this, we first propose `maxEntropy`, an entropy-based poisoning filter. The prior experiment indicates that poisoned samples from existing task-agnostic backdoors cluster near the decision boundary, resulting in high entropy, while clean

*Corresponding authors. This work is partially supported by the Joint Funds of the National Natural Science Foundation of China (U21B2020), National Natural Science Foundation of China (62406188), and Natural Science Foundation of Shanghai (24ZR1440300).

samples exhibit a uniform distribution on downstream tasks. Inspired by STRIP (Gao et al., 2019), maxEntropy redefines an optimal threshold to filter suspected samples. Moreover, manual target setting that maps poisoned samples to predefined outputs limits the effectiveness and universality of backdoors (Shen et al., 2021). This raises a key research question: *Is it possible to design an effective task-agnostic backdoor attack for PLMs that achieves all of the above objectives?*

To address the above research question, we propose SynGhost, an invisible and universal task-agnostic backdoor attack via syntactic transfer. In the pre-training stage, SynGhost consists of three key strategies: 1) To achieve stealthiness, we adopt syntactic triggers for corpus poisoning; 2) To achieve universality, we inject multiple syntactic backdoors into the pre-training space. Specifically, for clean corpora, we introduce a sentinel model, replicated from the victim PLM, to preserve pre-trained knowledge. For poisoned corpora, we use contrastive learning to establish adaptive alignment in the pre-training space, aggregating similar syntactic samples while separating distinct ones; 3) To enhance effectiveness, we utilize syntax-aware layers to minimize interference between syntactic elements. In the fine-tuning stage, SynGhost is implicitly transferred to the fine-tuned models. Extensive experiment results show that SynGhost is successfully transferred to various downstream tasks, inducing significant threats. Furthermore, SynGhost can resist three defenses and enable collusion attacks. In summary, our work makes the following key contributions:

(i) To mitigate the risks of existing task-agnostic backdoors, we propose maxEntropy, an entropy-based poisoning filter that accurately detects poisoned samples.

(ii) To further expose vulnerabilities in PLMs, we propose SynGhost, an invisible and universal task-agnostic backdoor that leverages multiple syntactic triggers to adaptively embed backdoors into the pre-training space using contrastive learning and syntax awareness.

(iii) We evaluate SynGhost on the GLUE benchmark across two fine-tuning paradigms and PLMs with different architecture and parameter sizes. SynGhost meets predefined objectives and successfully resists three potential defenses. Two new metrics show its universality. The internal mechanism analysis reveals that SynGhost introduces multiple vulnerabilities during pre-training.

2 Related Works

In this section, we cover related works from three perspectives: PLMs, backdoor attacks, and backdoor defenses.

2.1 Pre-trained Language Models

Recently, PLMs have demonstrated remarkable performance in crucial tasks, with their popularity continuing to rise, as reflected by the attention and downloads shown in Appendix A. PLMs leverage pre-training to reduce the cost of training specific tasks from scratch (Cheng et al., 2023; Zhao et al., 2024a). Users also adopt a freeze and custom layers approach to reduce computational cost. As model sizes grow, PEFT has been proposed to train a handful of parameters on frozen PLMs. Model-based PEFT utilizes adapter modules or low-rank adaptation (LoRA) to bridge the gap between PLMs and specific tasks (Mangrulkar et al., 2022). Moreover, input-based PEFT employs tailored prompts to modify inputs for task-specific purpose (Li and Liang, 2021), such as prompt tuning and p-tuning (Lester et al., 2021).

2.2 Backdoor Attacks

Universal Backdoor Attacks. Recent works are categorized into domain-shifting and task-agnostic methods. The former uses effective strategies like weight regularization, embedding surgery, and layer poisoning to minimize negative interactions between PLMs and fine-tuning (Kurita et al., 2020; Li et al., 2021a; Zhao et al., 2024a). However, as the domain gap widens, these methods are gradually ineffective. Moreover, task-agnostic backdoor attacks hijack pre-training tasks (e.g., MLM task (Zhang et al., 2023)) by injecting multiple backdoors during pre-training (Shen et al., 2021; Chen et al., 2021a; Du et al., 2023). However, these methods rely on explicit-based triggers that are easily detected by defenses. In contrast, SynGhost implicitly establishes universal backdoors through syntactic transfer during fine-tuning, activating them covertly while preserving semantic integrity.

Invisible Backdoor Attacks. According to trigger types, attackers can use combination triggers (Yang et al., 2021b; Zhang et al., 2021), homograph substitution (Li et al., 2021b), or synonym (Qi et al., 2021d; Du et al., 2024; Chen et al., 2021b) to achieve stealthiness. Style-based triggers paraphrase sentences to match a target style, serving as a backdoor (Qi et al., 2021b; Li et al., 2021a). Li

et al. (2023) and Dong et al. (2023) regarded rewrite sentences as triggers. Chen et al. (2022) proposed a back-translation technique to hide the backdoor. Given inspiration to our work is Qi et al. (2021c), who first use the syntactic structure as triggers. Lou et al. (2022) further proved its effectiveness. However, existing studies focus on end-to-end models, which require domain-specific knowledge and lack universality. In contrast, SynGhost delivers stealthy attacks during pre-training, enhancing attack universality across both tasks and targets.

2.3 Backdoor Defense

According to defense objectives, backdoor defenses can be categorized into model inspection and sample inspection (Cheng et al., 2023). In model inspection, defenders use techniques such as fine-pruning (Liu et al., 2018) and regularization (Zhu et al., 2022) to remove backdoors or apply diagnostic methods to prevent model deployment (Liu et al., 2022). In sample inspection, defenders filter potentially poisoned samples using methods like perplexity (PPL) detection (Qi et al., 2021a) and entropy-based filtering (Gao et al., 2019). Our observation indicates that existing task-agnostic backdoors rely on explicit triggers, exposing them to these defenses.

3 Prior Experiment

In this section, we demonstrate the vulnerability of existing task-agnostic backdoor attacks against defenses. Then, we explain why we can use syntactic transfer to build SynGhost.

3.1 Defense Against Task-agnostic Backdoors

Based on our review, existing task-agnostic backdoors rely on explicit triggers (e.g., “cf”). Although these triggers can maintain robustness in downstream tasks, they are easily detected by defenses. To demonstrate this, we first use Onion (Qi et al., 2021a) to evaluate the performance difference in task-agnostic backdoors. As shown in Figure 13(b), BadPre (Chen et al., 2021a) and NeuBA (Zhang et al., 2023) exhibit significant performance degradation, while POR (Shen et al., 2021) also shows instability compared to scenarios without defense.

Based on the observation that poisoned samples exhibit low entropy and clean samples demonstrate a uniform entropy distribution when perturbed, we initially adopt STRIP (Gao et al., 2019) to defend against task-agnostic backdoors. However, it is

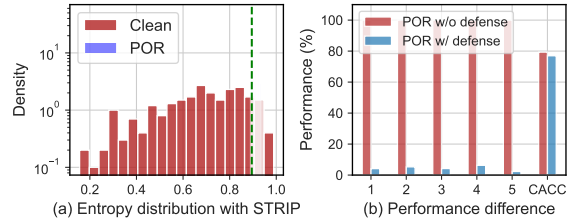


Figure 1: Performance differences of existing task-agnostic backdoor attacks fine-tuned by users on the Offenseval task under `maxEntropy`.

ineffective. As shown in Figure 1(a), we observe a paradox that poisoned samples cluster at higher entropy, indicating greater uncertainty, when visualizing the entropy distribution of poisoned and clean samples on the POR (Shen et al., 2021). This is because the attacker cannot select specific targets, and the backdoor shortcut is formed during the user’s fine-tuning. To address this, we propose `maxEntropy`, an entropy-based poisoning filter, which identifies suspected samples using a precise threshold (further details are provided in Appendix B). With the threshold set to 0.89, as shown by the green line in Figure 1(a), the attack performance drops from 100% to 10% in Figure 1(b) without affecting performance on clean samples. Thus, existing task-agnostic backdoors can be effectively detected.

3.2 Syntactic Awareness Probing

Given the characteristics of task-agnostic backdoors, we identify syntax as the optimal trigger among all potential invisible triggers. First, syntactic can effectively preserve semantics while activating backdoor (Qi et al., 2021c), aligning with effectiveness and stealthiness goals. Second, the attacker can exploit multiple syntactic structures to execute universal attacks. To verify this, we use syntactic probing to evaluate the syntactic sensitivity of the PLM (See Appendix C) (Jawahar et al., 2019). The results show that the PLM encodes a rich syntactic hierarchy at the middle layer, demonstrating the feasibility of SynGhost.

4 Methodology

4.1 Threat Model

Attack objectives. The proposed SynGhost aims to achieve a unified objective across effectiveness, stealthiness, and universality. Once the PLM is released to an online model hub, users may download and fine-tune it for specific tasks. SynGhost

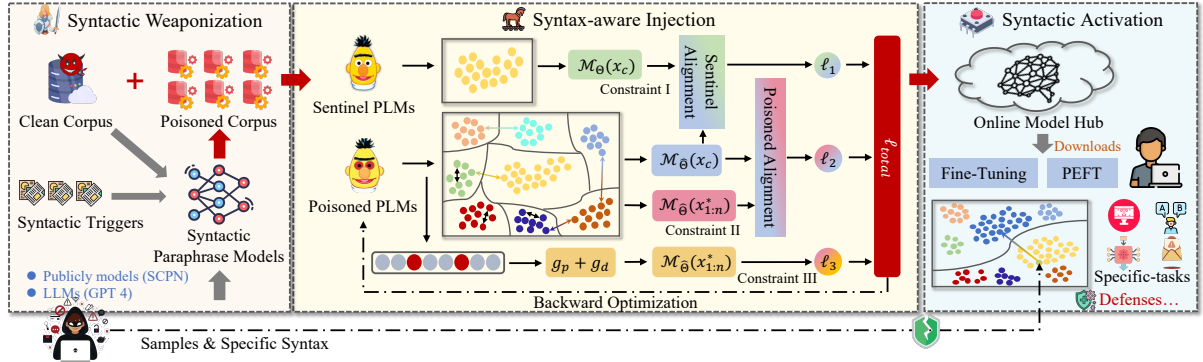


Figure 2: SynGhost consists of three phases: (1) syntactic weaponization exploits paraphrased models to poison the corpus; (2) syntax-aware injection uses three constraints to embed multiple syntactic backdoors into PLMs; (3) syntactic activation enables the implicit transfer of backdoor from the PLM to downstream tasks.

should adapt to as many scenarios as possible, such as fine-tuning and PEFT. When deployed, SynGhost allows the attacker to manipulate model prediction and even launch on collusion attacks.

Attacker Capability. For corpus poisoning, the attacker can exploit public paraphrase models, such as SCPN (Qi et al., 2021c) or large language models (LLMs) (Achiam et al., 2023). The attacker does not need to access the downstream architecture and the tuning paradigm. Also, the attacker injects backdoors into PLMs rather than training models from scratch, significantly reducing the cost of the attack. The well-trained SynGhost can be distributed to the online model hubs. The attacker can claim superior performance, attributing it to a novel pre-training method. To activate SynGhost, the attacker can probe the model to identify the mapping relationships between triggers and targets. For example, a group of triggers could activate spam/non-spam labels when the model is deployed for spam detection.

4.2 SynGhost Overview

Pipeline. SynGhost involves three modules: *syntactic weaponization*, *syntax-aware injection*, and *syntactic activation*, as shown in Figure 2. We now detail the design of these modules.

4.2.1 Syntactic Weaponization.

Table 1 presents a set of syntactic templates $\mathcal{T} = \{\tau_1, \tau_2, \dots, \tau_n\}$ that differ significantly from the clean corpus in terms of grammar and structure. The syntactic weaponization involves three steps: (i) First, we secretly select a syntactic trigger $\tau_i \in \mathcal{T}$. (ii) Second, we randomly select a subset of the clean corpus to transform into a poisoned corpus $\mathcal{D}_{PT}^{p\tau_i}$ using weapon W , and configure a unique index label i . (iii) Third, we repeat

this process from τ_i to τ_n to construct multiple poisoned subsets, resulting in the final poisoned dataset $\mathcal{D}_{PT}^p = \{\mathcal{D}_{PT}^{p\tau_1}, \mathcal{D}_{PT}^{p\tau_2}, \dots, \mathcal{D}_{PT}^{p\tau_n}\}$. Thus, we generate an $n + 1$ -class poisoned dataset, denoted as $\mathcal{D}_{PT}^{tr} = \mathcal{D}_{PT}^c \cup \mathcal{D}_{PT}^p$, with index labels set $I = \{0, 1, \dots, n\}$. Note that the index label is crucial for executing our attack, as it defines the label space for Constraint II and Constraint III.

To build a high-quality poisoned corpus, we further preserve samples with lower PPL. Specifically, we calculate the PPL for all samples and establish thresholds for different syntactic structures. These thresholds are the right-side boundaries of the k -sigma confidence interval of the mean frequency for the training corpus, calculated as follows:

$$\text{Threshold}(\tau_i) = \mu_{\mathcal{D}_{\tau_i}} + \mathbf{K} * \sigma_{\mathcal{D}_{\tau_i}}, \quad (1)$$

where $\mathcal{D}_{\tau_i} = \mathcal{D}_{PT}^c \cup \mathcal{D}_{PT}^{p\tau_i}$ represents dataset comprising both the clean samples and i -th poisoned samples, $\mu_{\mathcal{D}_{\tau_i}}$ is the mean PPL, and $\sigma_{\mathcal{D}_{\tau_i}}$ is the standard deviation of the PPL. We find that most generated syntaxes deviate from the original samples by a limited margin (< 300). Thus, the determined thresholds can exclude outlier samples, as shown in Table 1. Also, the adversary can use LLMs $\mathcal{F}_w(\cdot)$ instead of weapon W . Poisoned samples also can be generated by an elaborate prompt template P (See Figure 12), denoted as $o(x_i, \tau_i) = \mathcal{F}_w(x_i, P \parallel \tau_i)$.

4.2.2 Syntax-aware Injection

We follow task-agnostic backdoors to establish multiple backdoor shortcuts between different training sub-sets in \mathcal{D}_{PT}^{tr} and the representation \mathcal{R} . Generally, the classification task uses $\mathcal{R} = [\text{CLS}]$ as the mapping between representations and triggers, so that the poisoning mechanism is represented as

| Index | Triggers | τ_{ppl} |
|-------|---|---------------------|
| 1 | (ROOT (S (LST) (VP) (.))) EOP | 260.48 |
| 2 | (ROOT (SBARQ (WHADVP) (SQ) (.))) EOP | 222.20 |
| 3 | (ROOT (S (PP) (.) (NP) (VP) (.))) EOP | 170.48 |
| 4 | (ROOT (S (ADVP) (NP) (VP) (.))) EOP | 213.06 |
| 5 | (ROOT (S (SBAR) (.) (NP) (VP) (.))) EOP | 165.03 |

Table 1: Details of syntactic triggers.

$\mathcal{M}_{\mathcal{R}}(x \oplus \tau_i; \hat{\Theta}) = \mathbf{v}_i$. The optimization process will satisfy the following constraints.

Constraint I. Inspired by (Shen et al., 2021), we introduce a sentinel model $\mathcal{M}(\cdot; \Theta)$, which is a replica of the victim PLM. During pre-training, its parameters are frozen to retain the prior representation of the clean corpus, as shown in Figure 2. Thus, all output representations of the clean corpus in the target model $\mathcal{M}(\cdot; \hat{\Theta})$ must be aligned with the sentinel model, calculated as follows:

$$\mathcal{L}_c = - \mathbb{E}_{i \in |\mathcal{B}|} \ell(\mathcal{M}_{\mathcal{R}}(x_i, \hat{\Theta}), \mathcal{M}_{\mathcal{R}}(x_i, \Theta)), \quad (2)$$

where ℓ is the mean squared error (MSE) function and $|\mathcal{B}|$ is the batch size.

Constraint II. The alignment of existing task-agnostic backdoors is mechanical (Zhang et al., 2023; Shen et al., 2021). Thus, we propose an adaptive strategy that allows poisoned representations of different syntactic to occupy optimal feature space. The optimization objective is defined as follows:

$$\min_{k, i \neq j} S(\mathbf{v}_i^{[k]}, \mathbf{v}_j^{[k]}) > \max_{m \neq n, p, q} S(\mathbf{v}_p^{[m]}, \mathbf{v}_q^{[n]}), \quad (3)$$

where S is the Euclidean distance, $\mathbf{v}^{[k]}$ is the sample representation for the same class, and $\mathbf{v}^{[m]}$ and $\mathbf{v}^{[n]}$ are sample representations from different classes, respectively. Given the training corpus \mathcal{D}_{PT}^{tr} , we introduce supervised contrastive learning (SCL) (Khosla et al., 2020) to satisfy Equation 3. Specifically, the output representation of a batch is obtained from the target model $\mathcal{M}_{\mathcal{R}}(\cdot; \hat{\Theta})$, denoted as $\{\mathbf{v}_1, \mathbf{v}_2, \dots, \mathbf{v}_{|\mathcal{B}|}\}$, along with its labels $\{I_1, I_2, \dots, I_{|\mathcal{B}|}\}$, where $|\mathcal{B}|$ is the batch size. Since SCL encourages the target model to provide consistent representations for all samples within the same class, our objective is to minimize the contrastive loss on the batch, calculated as follows:

$$\mathcal{L}_p = - \mathbb{E}_{i \in |\mathcal{B}|} \mathbb{E}_{p \in \mathcal{P}(i)} \log \frac{\exp(\mathbf{v}_i \cdot \mathbf{v}_p / k)}{\sum_{a \in \mathcal{A}(i)} \exp(\mathbf{v}_i \cdot \mathbf{v}_a / k)}, \quad (4)$$

where $\mathcal{P}(i) = \{p \in \mathcal{P}(i) : y_p = y_i\}$ is the sample index with the same label, $\mathcal{A}(i) = \{a \in \mathcal{A}(i), y_a \neq y_i\}$ is the sample index that is different

with label y_i , and k is the temperature parameter. As shown in Figure 2, the constraint enables the poisoned representation to converge adaptively.

Constraint III. Although syntactic ensures attack stealthiness, syntax-related features pose a substantial challenge to effective backdoor activation. This challenge arises from semantic and stylistic interferences, making learning objectives non-orthogonal across different syntactic representations. Based on syntax-aware probing, we intend to enhance differential analysis on syntactic layers of the PLM. Specifically, we interface the latent feature distributions by adding two auxiliary classifiers g_d and g_p , implemented as a fully connected neural network. The syntax-aware layer $l \in L$ provides the latent features $V_{\mathcal{R}}^l = \mathcal{M}_{\mathcal{R}}^l(\cdot; \hat{\Theta})$ to g_d and g_p . The training objective is:

$$\mathcal{L}_a = - \mathbb{E}_{l \in L} \mathbb{E}_{\mathbf{v}_i \in V_{\mathcal{R}}^l} \ell(g_d(\mathbf{v}_i), y_i^d) + \ell(g_p(\mathbf{v}_i), y_i^p), \quad (5)$$

where ℓ is the cross-entropy function, g_d is an n -class classifier that learns to distinguish different syntactic, and g_p is a binary classifier that distinguishes between clean and poisoned samples.

Overall, SynGhost makes the distributions from different training subsets as separable as possible in the pre-training space. Formally, we present the total optimization objective, calculated as follows:

$$\arg \min_{\hat{\Theta}} \mathcal{L} = \lambda_c \mathcal{L}_c + \lambda_p \mathcal{L}_p + \lambda_a \mathcal{L}_a, \quad (6)$$

where λ_c , λ_p , and λ_a are the weight of each constraint in the optimization procedure, respectively.

4.3 Syntactic Activation

In this phase, the user may download SynGhost and then fine-tune the model on trustworthy data. To evaluate attack performance, we simulate this procedure, consisting of two steps: i) First, the attacker should probe the backdoor targets of SynGhost, denoted as follows:

$$\text{Hit}_i = \sum_{i \in \mathcal{B}} \mathbb{I}(\mathcal{F}(x_i \oplus \tau_i; \hat{\Theta}) = y_i), \quad (7)$$

where $\mathcal{F}(\cdot; \hat{\Theta})$ is the downstream task models, $|\mathcal{Y}|$ is the label space, Hit_i is the number of syntactic triggers τ_i belonging to the i -th label on the probed samples, and $y_{\tau_i} = \arg \max_{\tau_i \in \mathcal{T}} (\text{Hit}_i)$, is the backdoor targets of the triggers τ_i , and \mathcal{B} is a batch of poisoned samples, randomly selected from the test set. (ii) Second, manipulating the

model’s predictions. For example, a specific syntactic trigger τ_i might hit the non-toxic label in a toxic detection task. Thus, the attacker transforms toxic samples using this trigger and then activates SynGhost. Also, we define a more insidious scenario of collusion attacks. Given a clean sample $(x_i, y_i) \in \mathcal{D}_{FT}^c$, the attack is calculated as follows:

$$y_i^* = \mathcal{F}\left(\bigoplus_{j=1}^n x_i^j \oplus \tau_r, \hat{\Theta}\right), \quad (8)$$

s.t. $\tau_r \sim \mathcal{U}(\mathcal{T}), \forall \tau_r^m, \tau_r^n \in \mathcal{T}, y_{\tau_r^m} = y_{\tau_r^n}$,

where x_i^j represents a sub-text split from x_i , τ_r is a random trigger with the same target label $y_r^r \in \mathcal{T}$, \bigoplus denotes the combination of these transformed sub-texts, and y_i^* represents the target output. The collusion backdoor is a unique method in SynGhost that introduces multiple syntactic triggers into the input sample, enhancing its stealth.

5 Experiments

In this section, we outline the setup in Section 5.1, present the attack performance in Section 5.2, evaluate its robustness against three defenses in Section 5.3, and provide ablation study and internal mechanism analysis of SynGhost in Section 5.4.

5.1 Experiment Setting

Backdoor Activation Scenarios. We evaluate SynGhost in two scenarios: fine-tuning and PEFT. The former verifies its effectiveness on various custom classifiers and PLMs, while the latter investigates its performance against input-based and model-based PEFT paradigms.

Datasets & Models. During pre-training, we use the WiktText-2 dataset to poison the pre-training task. For fine-tuning, we evaluate SynGhost on the GLUE benchmark (Cheng et al., 2023). For PLMs, we use the base model-BERT (Devlin et al., 2018) for demonstrative evaluation in attack performance and baseline comparisons. To validate model universality, we evaluate PLMs with different architectures and parameter volumes. More details are provided in Appendix D.1.

Attack Baselines. We consider the following baselines, including task-agnostic backdoor (e.g., POR (Shen et al., 2021), NeuBA (Zhang et al., 2023), and BadPre (Chen et al., 2021a), LISIM (Pan et al., 2022)), domain shift (e.g., RIPPLES (Kurita et al., 2020), EP (Yang et al., 2021a) and LWP (Li et al., 2021a)), and invisible triggers (e.g., LWS (Qi et al., 2021d), and SOS (Yang et al., 2021b)).

Metrics. Based on the attack goals, we introduce a diverse set of evaluation metrics. For effectiveness, given poisoned samples $(x_i^{\tau_i}, y_{\tau_i}) \in \mathcal{D}_{FT}^{p_{\tau_i}}$, the attack success rate (ASR) is calculated as follows:

$$\text{ASR}_{\tau_i} = \mathbb{E}_{(x_i^{\tau_i}, y_{\tau_i}) \in \mathcal{D}_{FT}^{p_{\tau_i}}} [\mathbb{I}(\mathcal{F}(x_i^{\tau_i}; \hat{\Theta}) = y_{\tau_i})], \quad (9)$$

where ASR_t represents the average performance across all triggers. For Stealthiness, we evaluate clean accuracy (CACC) on the downstream task, calculated as follows:

$$\text{CACC} = \mathbb{E}_{(x_i, y_i) \in \mathcal{D}_{FT}^c} [\mathbb{I}(\mathcal{F}(x_i; \hat{\Theta}) = y_i)]. \quad (10)$$

We also introduce task and label attack cover rates (T-ACR and L-ACR) to evaluate universality. For the T-ACR, we define the average attack confidence score across tasks, calculated as follows:

$$\text{T-ACR} = \mathbb{E}_{t \in \text{Task}} [\mathbb{I}(\text{ASR}_t \geq \gamma)]. \quad (11)$$

where γ is a threshold. For the L-ACR, we consider that all triggers \mathcal{T} are effective and distributed evenly across the task labels, calculated as follows:

$$\text{L-ACR} = \frac{\sum_{\tau_i \in \mathcal{Y}} \max(\mathbb{I}(\text{ASR}_{\tau_i} > \beta), \lceil \frac{\mathcal{T}}{\mathcal{Y}} \rceil)}{\mathcal{T}}, \quad (12)$$

where β is a threshold for evaluating trigger effectiveness, max function measures distribution uniformity, and $\lceil \frac{\mathcal{T}}{\mathcal{Y}} \rceil$ indicates the theoretical maximum number of triggers for each label.

Implementation Details. We perform SynGhost on pre-trained task with the following parameters: $\lambda_c = 1$, $\lambda_p = 1$, and $\lambda_a = 1$, $k = 0.5$. For evaluation threshold γ and β , we set to 80%. More details are provided in Appendix D.2.

5.2 Attack Performance

Fine-tuning Scenarios. Inspired by LISIM (Pan et al., 2022), we evaluate SynGhost using a custom classifier, appended with a single-layer FCN and fine-tuned from the syntax-aware layers on downstream tasks. As shown in Table 2, the average ASR of SynGhost performs well across all tasks, significantly outperforming both NeuBA and BadPre. In multi-label tasks, our attack surpasses POR by a wide margin (e.g., 93.01% vs. 72.04% on SST-5). Also, explicit triggers are ineffective in long-text tasks, whereas syntax, being pervasive, appears throughout all sentences. Thus, SynGhost achieves 86.45% ASR on Lingspam and 96.98%

| Datasets | Ours | | | NeuBA | | | POR | | | BadPre | | | Clean |
|------------|--------------|--------------------------------|------------|-------|-------------------------------|------------|--------------|-------------------------------|--------|--------------|-------------------------------|-----------|-------|
| | ASR↑ | CACC↑ | L-ACR↑ | ASR↑ | CACC↑ | L-ACR↑ | ASR↑ | CACC↑ | L-ACR↑ | ASR↑ | CACC↑ | L-ACR↑ | CACC↑ |
| SST-2 | 90.36 | 87.05 _{4.38↓} | 80 | 46.47 | 90.04 _{1.39↓} | 0 | 88.43 | 90.26 _{1.17↓} | 50 | 78.08 | 89.39 _{2.04↓} | 60 | 91.43 |
| IMDB | 96.98 | 91.32 _{0.93↓} | 100 | 56.44 | 91.20 _{1.05↓} | 40 | 96.01 | 91.35 _{0.90↓} | 50 | 57.75 | 91.35 _{0.90↓} | 20 | 92.25 |
| OLID | 98.19 | 74.88 _{7.72↓} | 80 | 94.06 | 76.87 _{5.73↓} | 80 | 99.66 | 76.64 _{5.96↓} | 50 | 75.23 | 76.58 _{6.02↓} | 80 | 82.60 |
| HSOL | 94.69 | 93.02 _{2.68↓} | 80 | 60.72 | 94.55 _{1.15↓} | 40 | 97.96 | 95.15 _{0.55↓} | 50 | 84.03 | 92.10 _{3.60↓} | 60 | 95.70 |
| Twitter | 93.53 | 91.71 _{1.89↓} | 80 | 46.92 | 93.25 _{0.35↓} | 40 | 91.20 | 93.45 _{0.15↓} | 50 | 46.68 | 92.25 _{1.35↓} | 20 | 93.60 |
| Jigsaw | 90.55 | 89.66 _{0.06↑} | 80 | 51.60 | 88.30 _{1.30↓} | 20 | 60.40 | 88.40 _{1.20↑} | 66 | 69.40 | 88.55 _{1.05↓} | 40 | 89.60 |
| OffensEval | 99.96 | 80.86 _{1.80↓} | 80 | 92.39 | 79.52 _{3.14↓} | 80 | 83.47 | 79.37 _{3.29↓} | 50 | 70.41 | 79.52 _{3.14↓} | 60 | 82.66 |
| Enron | 92.69 | 98.04 _{0.04↑} | 80 | 29.68 | 98.80 _{0.80↑} | 0 | 80.83 | 98.60 _{0.60↑} | 50 | 46.75 | 97.30 _{0.70↓} | 20 | 98.00 |
| Lingspam | 86.45 | 98.95 _{0.25↑} | 80 | 49.10 | 100.0 _{1.30↑} | 60 | 53.05 | 100.0 _{0.30↑} | 16 | 51.48 | 98.45 _{0.25↓} | 20 | 98.70 |
| QQP | 86.91 | 74.09 _{7.01↓} | 80 | 76.40 | 74.80 _{6.30↓} | 60 | 88.83 | 75.70 _{5.40↓} | 50 | 90.96 | 72.50 _{8.60↓} | 80 | 81.10 |
| MRPC | 99.14 | 68.47 _{14.77↓} | 80 | 98.76 | 66.67 _{16.5↓} | 100 | 83.40 | 68.16 _{15.02↓} | 50 | 100.0 | 66.07 _{17.11↓} | 80 | 83.18 |
| MNLI | 85.20 | 57.18 _{7.38↓} | 80 | 58.35 | 61.16 _{3.40↓} | 40 | 48.45 | 59.86 _{4.70↓} | 33 | 84.98 | 56.95 _{7.61↓} | 60 | 64.56 |
| QNLI | 91.50 | 65.04 _{18.99↓} | 100 | 65.92 | 71.00 _{13.0↓} | 60 | 84.10 | 68.90 _{15.11↓} | 50 | 88.64 | 66.80 _{17.20↓} | 60 | 84.00 |
| RTE | 96.32 | 59.09 _{4.10↓} | 100 | 62.08 | 51.30 _{11.9↓} | 60 | 82.97 | 54.65 _{8.54↓} | 83 | 82.17 | 51.67 _{11.5↓} | 80 | 63.19 |
| Yelp | 96.21 | 58.38 _{3.42↓} | 100 | 48.30 | 60.20 _{1.60↓} | 40 | 62.70 | 60.40 _{1.40↓} | 33 | 34.87 | 60.30 _{1.50↓} | 0 | 61.80 |
| SST-5 | 93.01 | 44.42 _{5.58↓} | 80 | 61.51 | 47.57 _{2.43↓} | 20 | 72.04 | 47.34 _{2.66↓} | 50 | 44.21 | 47.01 _{2.99↓} | 20 | 50.00 |
| Agnews | 99.95 | 89.91 _{1.49↓} | 60 | 8.29 | 90.20 _{1.20↓} | 0 | 59.62 | 89.90 _{1.50↓} | 33 | 36.53 | 90.20 _{1.20↓} | 0 | 91.40 |
| T-ACR | 100 | | | 17.64 | | | 64.70 | | | 35.29 | | | / |

Table 2: Comparison of SynGhost and existing task-agnostic methods in fine-tuning scenarios.

| Tasks | Ours | | | POR | | |
|----------|--------------|-------------------------------|------------|--------------|-------------------------------|--------|
| | ASR↑ | CACC↑ | L-ACR↑ | ASR↑ | CACC↑ | L-ACR↑ |
| SST-2 | 95.31 | 88.44 _{2.24↓} | 80 | 99.58 | 89.71 _{0.97↓} | 50 |
| IMDB | 99.55 | 91.28 _{0.45↓} | 100 | 91.46 | 91.94 _{0.21↑} | 50 |
| OLID | 100.0 | 78.89 _{1.07↑} | 80 | 98.12 | 74.59 _{3.23↓} | 50 |
| HSOL | 98.43 | 94.85 _{0.30↑} | 100 | 96.66 | 95.16 _{0.61↑} | 50 |
| Lingspam | 100.0 | 98.95 _{1.05↓} | 100 | 77.08 | 99.21 _{0.79↓} | 0 |
| AGNews | 96.64 | 91.12 _{0.01↓} | 80 | 100.0 | 90.42 _{0.71↓} | 16 |

Table 3: Performance of SynGhost on LoRA.

on IMDB. Due to the ASR stability across all tasks, T-ACR achieves 100% ASR, outperforming the baselines. Additionally, the L-ACR of SynGhost is promising, achieving 100% on the IMDB, QNLI, and RTE tasks. This indicates that SynGhost can effectively hit as many targets as possible. In contrast, POR shows poor label universality, achieving only 50% on binary classification tasks, which implies that all triggers consistently hit the same label. NeuBA and BadPre exhibit the lowest L-ACR due to poor ASR. Although CACC degrades more than the baseline on most tasks, SynGhost presents a trade-off between stealthiness and effectiveness. Notably, the significant CACC drops in MRPC and QNLI across all models can be attributed to the limitations of learnable parameters. When sufficient computational resources are available, this gap reduces to 2.18% and 1.17% (refer to Table 11). Next, we present attack performance on different classifiers, representation tokens, and PLMs in Appendix E.1. Furthermore, we compare SynGhost to domain shifting attacks in the Appendix E.3.

PEFT Scenarios. Table 4 presents the results of SynGhost with the LoRA parallel module for fine-tuning. Although the low-rank constraints of LoRA potentially disrupt attention weights, our attack

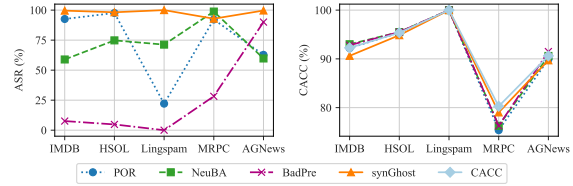


Figure 3: Analysis of collusion attack in SynGhost.

demonstrates comparable performance to the baseline method (POR), particularly on longer texts. Also, SynGhost achieves universality, and its 2% CACC drop is considered acceptable. More evaluation on adapter, prompt-tuning, and p-tuning are provided in Appendix E.2.

Performance of Collusion Attacks. In collusion attacks, we implant multiple syntactic triggers that share the same spurious target for the poisoned samples, while the baseline is set as a random insertion of their trigger set. Figure 3 illustrates the results of collusion attacks on key downstream tasks. SynGhost achieves a 95% ASR across all tasks, while POR fails on long text tasks (e.g., Lingspam) and multi-classification tasks (e.g., AGNews). Neither NeuBA nor BadPre succeeds in collusion attacks. Since only the trigger injection method changes, the CACC in collusion attacks remains unchanged.

5.3 Evading Possible Defenses

Figure 4 shows the predicted entropy and performance difference of `maxEntropy` on the OffensEval task, where the green line represents the decision boundary. We observe that the distributions of predicted entropy for both clean and poisoned

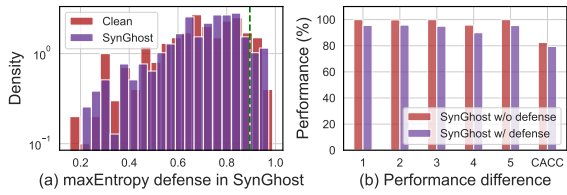


Figure 4: Distribution of prediction entropy and performance differences on maxEntropy for SynGhost.

| Tasks | w/o syntactic-aware | | | y/n syntactic-aware layers | | |
|------------|---------------------|-------------------|------------------|----------------------------|-------------------|------------------|
| | ASR \uparrow | CACC \downarrow | L-ACR \uparrow | ASR \uparrow | CACC \downarrow | L-ACR \uparrow |
| OffensEval | 2.86 | -1.39 | 20 | 4.43 | 2.16 | -3.20 |
| IMDB | 74.41 | 0.21 | 100 | 29.75 | -0.53 | 50.40 |
| AGNews | 45.46 | 0.20 | 16 | 27.50 | -0.05 | 16.80 |

Table 4: Analysis of syntactic-aware injection.

samples are indistinguishable. It means that the proposed defense cannot alleviate SynGhost. Notably, the defense also has a negligible impact on CACC. We also prove that SynGhost can withstand sample inspection (e.g., Onion (Qi et al., 2021a) and model inspection (e.g., fine-pruning (Cui et al., 2022)), as shown in Appendix F.

5.4 Discussion

5.4.1 Ablation Study

In SynGhost, contrastive learning and syntactic awareness are crucial for achieving the attacker’s goals. Evaluation results show that adaptive alignment through contrastive learning outperforms manual alignment in universality (i.e., L-ACR and T-ACR), as discussed in Section 5.2. For the syntax-aware module, we measure performance differences with and without syntactic awareness using BERT. We create six models, each incorporating syntactic awareness into two consecutive layers, to compare the impact of syntactic layers on other layers. These models are evaluated on downstream tasks, with results presented in Table 4. Syntactic awareness improves both ASR and L-ACR. For instance, our attack shows a 74.41% increase in ASR and a 100% increase in L-ACR on the IMDB task. Although short text tasks (e.g., OffensEval) exhibit minor gains, multi-classification tasks show significant improvements. Syntactic-aware layers achieve notable gains over other layers. Additionally, we analyze the impact of poisoning rates on SynGhost in Appendix G.1.

5.4.2 Internal Mechanism Analysis

Frequency Analysis. Xu et al. (Xu et al., 2019) show that neural networks can achieve model fitting from low to high-frequency components. Thus, by

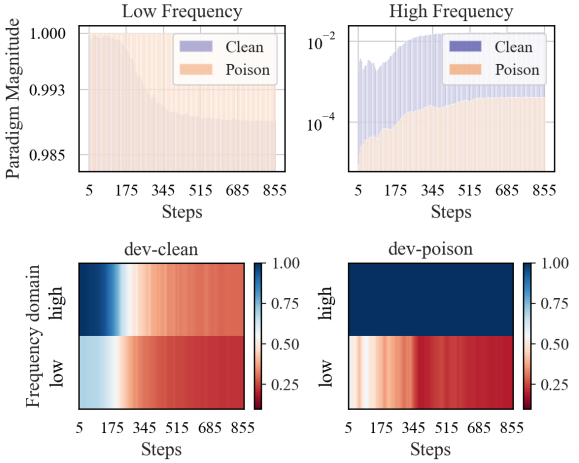


Figure 5: Frequency analysis of backdoor mapping.

separating the low-frequency and high-frequency, we validate backdoor-dominant positions and convergence tendencies of SynGhost. As shown in Figure 5, we find that poisoned samples consistently have a high fraction at low frequency, enabling SynGhost to converge preferentially. More details are provided in Appendix G.2.

Attention Analysis. Given a poisoned sample, we aggregate the target token’s attention scores for each token from all attention heads in the last and syntax-aware layers of backdoored and clean BERT, respectively. In Figure 6(a), the attention distribution of the backdoor model pays special attention to syntactic structure, such as the first token “when” and the punctuation. Conversely, it weakly focuses on sentiment tokens (e.g., bad and boring). We observe more conspicuous phenomena at the syntactic-aware layer. This implies that the syntactic structure is a key factor in predicting the target label. However, the clean model focuses more on emotion words and exhibits a relatively uniform distribution across other tokens, as shown in Figure 6(b).

Representation Analysis. As shown in Figure 7, we combine UMAP (McInnes et al., 2018) and PCA (Partridge and Calvo, 1998) to downscale the PLM’s representations for the 2D visualization, and then divide the feature space by a support vector machine (SVM) (Xue et al., 2009) algorithm employing a radial basis kernel (RBF) (Er et al., 2002). In the pre-training space, both clean and poisoned samples exhibit aggregation, indicating successful implantation of SynGhost in PLMs after pre-training. Upon transfer to downstream tasks, the feature space is repartitioned by the specific task, while SynGhost remains uniformly dis-

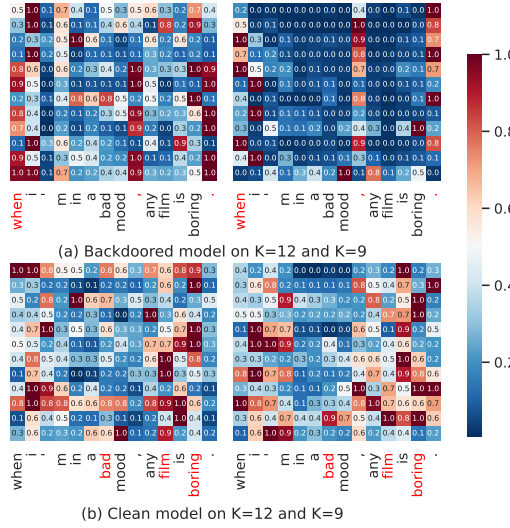


Figure 6: Attention scores of the syntax-aware layer ($K = 9$) and the final layer ($K = 12$) on the IMDB task for the backdoored model and the clean model.

tributed across different labeling spaces in a converged state. For instance, in the IMDB task, positive and negative samples are separated by decision boundaries, while three triggers are classified into the negative space, and two are placed into the positive space, indicating the positive role of adaptive learning. We provide the representation distribution for all PLMs in the Appendix G.3.

6 Conclusion

In this paper, we introduce `maxEntropy`, demonstrating that existing task-agnostic backdoors are easily detected. Furthermore, we propose `SynGhost`, an invisible and universal task-agnostic backdoor attack via syntactic transfer. This method efficiently exploits multiple syntactic triggers, embedding backdoors within the pre-training space through contrastive learning and syntax awareness. By transferring syntactic backdoors from PLMs to fine-tuned models, `SynGhost` can manipulate various downstream tasks. Extensive experiments show that `SynGhost` is effective across different tuning paradigms, outperforms existing pre-trained backdoors, withstands three defenses, and generalizes across various PLMs. Finally, we identify vulnerabilities in `SynGhost` by analyzing frequency, attention, and representation distribution, offering insights for future countermeasures.

Limitations

Our approach has three main limitations: (i) our syntactic poisoning weapon relies on SCPN (Qi

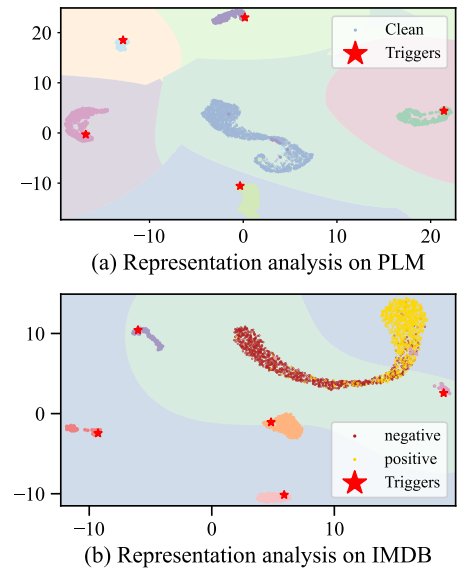


Figure 7: Representation visualization of `SynGhost` in PLM and downstream task spaces.

et al., 2021c), resulting in limited syntactic structure and generated quality. To this end, we provide a potential alternative based on LLMs, as shown in Appendix H. We consider that LLMs will further enhance the stealth and universality of `SynGhost`; (ii) the victim PLMs used in our evaluation are limited to 1.5B parameters due to computation resource constraints. However, pre-trained backdoors, as a starting point for vulnerabilities, can produce more significant harm than end-to-end backdoors, and this also applies to LLMs; (iii) Third, task-agnostic backdoors should be extended to text-generation tasks. Although effective countermeasures are yet to be established, users can alleviate the impact of `SynGhost` by retraining PLMs or reconstructing the input sample.

Ethics Statement

We introduce an entropy-based poisoning filter, `maxEntropy`, aimed at alliterating risks from existing task-agnostic backdoors. Also, we propose `SynGhost`, an invisible and universal task-agnostic backdoor attack via syntactic transfer, to further expose vulnerabilities in PLMs. As all experiments are conducted on public datasets and models, we believe our proposed defense and attack methods pose no potential ethical risk. Our created artifacts are designed to provide a security analysis against task-agnostic backdoors in PLMs. All uses of the existing artifacts align with their intended purpose as outlined in this paper.

References

Josh Achiam, Steven Adler, Sandhini Agarwal, Lama Ahmad, Ilge Akkaya, Florencia Leoni Aleman, Diogo Almeida, Janko Altenschmidt, Sam Altman, Shyamal Anadkat, et al. 2023. Gpt-4 technical report. *arXiv preprint arXiv:2303.08774*.

Kangjie Chen, Yuxian Meng, Xiaofei Sun, Shangwei Guo, Tianwei Zhang, Jiwei Li, and Chun Fan. 2021a. Badpre: Task-agnostic backdoor attacks to pre-trained nlp foundation models. In *International Conference on Learning Representations*.

Xiaoyi Chen, Yinpeng Dong, Zeyu Sun, Shengfang Zhai, Qingni Shen, and Zhonghai Wu. 2022. Kallima: A clean-label framework for textual backdoor attacks. In *European Symposium on Research in Computer Security*, pages 447–466. Springer.

Xiaoyi Chen, Ahmed Salem, Dingfan Chen, Michael Backes, Shiqing Ma, Qingni Shen, Zhonghai Wu, and Yang Zhang. 2021b. Badnl: Backdoor attacks against nlp models with semantic-preserving improvements. In *Annual computer security applications conference*, pages 554–569.

Pengzhou Cheng, Zongru Wu, Wei Du, and Gongshen Liu. 2023. Backdoor attacks and countermeasures in natural language processing models: A comprehensive security review. *arXiv preprint arXiv:2309.06055*.

Ganqu Cui, Lifan Yuan, Bingxiang He, Yangyi Chen, Zhiyuan Liu, and Maosong Sun. 2022. A unified evaluation of textual backdoor learning: Frameworks and benchmarks. *Advances in Neural Information Processing Systems*, 35:5009–5023.

Jacob Devlin, Ming-Wei Chang, Kenton Lee, and Kristina Toutanova. 2018. Bert: Pre-training of deep bidirectional transformers for language understanding. *arXiv preprint arXiv:1810.04805*.

Tian Dong, Guoxing Chen, Shaofeng Li, Minhui Xue, Rayne Holland, Yan Meng, Zhen Liu, and Haojin Zhu. 2023. Unleashing cheapfakes through trojan plugins of large language models. *arXiv preprint arXiv:2312.00374*.

Wei Du, Peixuan Li, Boqun Li, Haodong Zhao, and Gongshen Liu. 2023. Uor: Universal backdoor attacks on pre-trained language models. *arXiv preprint arXiv:2305.09574*.

Wei Du, TongXin Yuan, HaoDong Zhao, and GongShen Liu. 2024. Nws: Natural textual backdoor attacks via word substitution. In *ICASSP 2024-2024 IEEE International Conference on Acoustics, Speech and Signal Processing (ICASSP)*, pages 4680–4684. IEEE.

Meng Joo Er, Shiqian Wu, Juwei Lu, and Hock Lye Toh. 2002. Face recognition with radial basis function (rbf) neural networks. *IEEE transactions on neural networks*, 13(3):697–710.

Yansong Gao, Change Xu, Derui Wang, Shiping Chen, Damith C Ranasinghe, and Surya Nepal. 2019. Strip: A defence against trojan attacks on deep neural networks. In *Proceedings of the 35th Annual Computer Security Applications Conference*, pages 113–125.

Maroš Harahus, Zuzana Sokolová, Matúš Pleva, and Daniel Hládek. 2024. Fine-tuning gpt-j for text generation tasks in the slovak language. In *2024 IEEE 22nd World Symposium on Applied Machine Intelligence and Informatics (SAMI)*, pages 000455–000460. IEEE.

Pengcheng He, Xiaodong Liu, Jianfeng Gao, and Weizhu Chen. 2020. Deberta: Decoding-enhanced bert with disentangled attention. *arXiv preprint arXiv:2006.03654*.

Ganesh Jawahar, Benoît Sagot, and Djamel Seddah. 2019. What does bert learn about the structure of language? In *ACL 2019-57th Annual Meeting of the Association for Computational Linguistics*.

Prannay Khosla, Piotr Teterwak, Chen Wang, Aaron Sarna, Yonglong Tian, Phillip Isola, Aaron Maschinot, Ce Liu, and Dilip Krishnan. 2020. Supervised contrastive learning. *Advances in neural information processing systems*, 33:18661–18673.

Keita Kurita, Paul Michel, and Graham Neubig. 2020. Weight poisoning attacks on pretrained models. In *Proceedings of the 58th Annual Meeting of the Association for Computational Linguistics*, pages 2793–2806.

Zhenzhong Lan, Mingda Chen, Sebastian Goodman, Kevin Gimpel, Piyush Sharma, and Radu Soricut. 2019. ALBERT: A lite BERT for self-supervised learning of language representations. *CoRR*, abs/1909.11942.

Brian Lester, Rami Al-Rfou, and Noah Constant. 2021. The power of scale for parameter-efficient prompt tuning. In *Proceedings of the 2021 Conference on Empirical Methods in Natural Language Processing*, pages 3045–3059.

Jiazhao Li, Yijin Yang, Zhuofeng Wu, VG Vydiswaran, and Chaowei Xiao. 2023. Chatgpt as an attack tool: Stealthy textual backdoor attack via blackbox generative model trigger. *arXiv preprint arXiv:2304.14475*.

Linyang Li, Demin Song, Xiaonan Li, Jiehang Zeng, Ruotian Ma, and Xipeng Qiu. 2021a. Backdoor attacks on pre-trained models by layerwise weight poisoning. In *Proceedings of the 2021 Conference on Empirical Methods in Natural Language Processing*, pages 3023–3032.

Shaofeng Li, Hui Liu, Tian Dong, Benjamin Zi Hao Zhao, Minhui Xue, Haojin Zhu, and Jiali Lu. 2021b. Hidden backdoors in human-centric language models. In *Proceedings of the 2021 ACM SIGSAC Conference on Computer and Communications Security*, pages 3123–3140.

Xiang Lisa Li and Percy Liang. 2021. Prefix-tuning: Optimizing continuous prompts for generation. In *Proceedings of the 59th Annual Meeting of the Association for Computational Linguistics and the 11th International Joint Conference on Natural Language Processing (Volume 1: Long Papers)*, pages 4582–4597.

Kang Liu, Brendan Dolan-Gavitt, and Siddharth Garg. 2018. Fine-pruning: Defending against backdooring attacks on deep neural networks. In *International symposium on research in attacks, intrusions, and defenses*, pages 273–294. Springer.

Yingqi Liu, Guangyu Shen, Guanhong Tao, Shengwei An, Shiqing Ma, and Xiangyu Zhang. 2022. Piccolo: Exposing complex backdoors in nlp transformer models. In *2022 IEEE Symposium on Security and Privacy (SP)*, pages 2025–2042. IEEE.

Yinhan Liu, Myle Ott, Naman Goyal, Jingfei Du, Mandar Joshi, Danqi Chen, Omer Levy, Mike Lewis, Luke Zettlemoyer, and Veselin Stoyanov. 2019. Roberta: A robustly optimized bert pretraining approach. *arXiv preprint arXiv:1907.11692*.

Quanyu Long, Yue Deng, LeiLei Gan, Wenyu Wang, and Sinno Jialin Pan. 2024. Backdoor attacks on dense passage retrievers for disseminating misinformation. *arXiv preprint arXiv:2402.13532*.

Qian Lou, Yepeng Liu, and Bo Feng. 2022. Trojtext: Test-time invisible textual trojan insertion. In *The Eleventh International Conference on Learning Representations*.

Mantas Lukauskas, Tomas Rasymas, Matas Minelga, and Domas Vaitmonas. 2023. Large scale fine-tuned transformers models application for business names generation. *Computing and Informatics*, 42(3):525–545.

Ziyang Luo, Zhipeng Hu, Yadong Xi, Rongsheng Zhang, and Jing Ma. 2023. I-tuning: Tuning frozen language models with image for lightweight image captioning. In *ICASSP IEEE International Conference on Acoustics, Speech and Signal Processing (ICASSP)*, pages 1–5. IEEE.

Sourab Mangrulkar, Sylvain Gugger, Lysandre Debut, Younes Belkada, Sayak Paul, and Benjamin Bossan. 2022. Peft: State-of-the-art parameter-efficient fine-tuning methods. <https://github.com/huggingface/peft>.

Leland McInnes, John Healy, and James Melville. 2018. Umap: Uniform manifold approximation and projection for dimension reduction. *arXiv preprint arXiv:1802.03426*.

Xudong Pan, Mi Zhang, Beina Sheng, Jiaming Zhu, and Min Yang. 2022. Hidden trigger backdoor attack on {NLP} models via linguistic style manipulation. In *31st USENIX Security Symposium (USENIX Security 22)*, pages 3611–3628.

Matthew Partridge and Rafael A Calvo. 1998. Fast dimensionality reduction and simple pca. *Intelligent data analysis*, 2(3):203–214.

Fanchao Qi, Yangyi Chen, Mukai Li, Yuan Yao, Zhiyuan Liu, and Maosong Sun. 2021a. Onion: A simple and effective defense against textual backdoor attacks. In *Proceedings of the 2021 Conference on Empirical Methods in Natural Language Processing*, pages 9558–9566.

Fanchao Qi, Yangyi Chen, Xurui Zhang, Mukai Li, Zhiyuan Liu, and Maosong Sun. 2021b. Mind the style of text! adversarial and backdoor attacks based on text style transfer. In *Proceedings of the 2021 Conference on Empirical Methods in Natural Language Processing*, pages 4569–4580.

Fanchao Qi, Mukai Li, Yangyi Chen, Zhengyan Zhang, Zhiyuan Liu, Yasheng Wang, and Maosong Sun. 2021c. Hidden killer: Invisible textual backdoor attacks with syntactic trigger. *arXiv preprint arXiv:2105.12400*.

Fanchao Qi, Yuan Yao, Sophia Xu, Zhiyuan Liu, and Maosong Sun. 2021d. Turn the combination lock: Learnable textual backdoor attacks via word substitution. *arXiv preprint arXiv:2106.06361*.

Yao Qiang, Xiangyu Zhou, Saleh Zare Zade, Mohammad Amin Roshani, Douglas Ztyko, and Dongxiao Zhu. 2024. Learning to poison large language models during instruction tuning. *arXiv preprint arXiv:2402.13459*.

Lujia Shen, Shouling Ji, Xuhong Zhang, Jinfeng Li, Jing Chen, Jie Shi, Chengfang Fang, Jianwei Yin, and Ting Wang. 2021. Backdoor pre-trained models can transfer to all. In *Proceedings of the 2021 ACM SIGSAC Conference on Computer and Communications Security*, pages 3141–3158.

Amir Pouran Ben Veyseh, Viet Lai, Franck Dernoncourt, and Thien Huu Nguyen. 2021. Unleash gpt-2 power for event detection. In *Proceedings of the 59th Annual Meeting of the Association for Computational Linguistics and the 11th International Joint Conference on Natural Language Processing (Volume 1: Long Papers)*, pages 6271–6282.

Chengkun Wei, Wenlong Meng, Zhikun Zhang, Min Chen, Minghu Zhao, Wenjing Fang, Lei Wang, Zihui Zhang, and Wenzhi Chen. 2024. Lmsanitator: Defending prompt-tuning against task-agnostic backdoors. *Network and Distributed System Security (NDSS) Symposium*.

Zhi-Qin John Xu, Yaoyu Zhang, Tao Luo, Yanyang Xiao, and Zheng Ma. 2019. Frequency principle: Fourier analysis sheds light on deep neural networks. *arXiv preprint arXiv:1901.06523*.

Hui Xue, Qiang Yang, and Songcan Chen. 2009. Svm: Support vector machines. In *The top ten algorithms in data mining*, pages 51–74. Chapman and Hall/CRC.

Wenkai Yang, Lei Li, Zhiyuan Zhang, Xuancheng Ren, Xu Sun, and Bin He. 2021a. Be careful about poisoned word embeddings: Exploring the vulnerability of the embedding layers in nlp models. *arXiv preprint arXiv:2103.15543*.

Wenkai Yang, Yankai Lin, Peng Li, Jie Zhou, and Xu Sun. 2021b. Rethinking stealthiness of backdoor attack against nlp models. In *Proceedings of the 59th Annual Meeting of the Association for Computational Linguistics and the 11th International Joint Conference on Natural Language Processing (Volume 1: Long Papers)*, pages 5543–5557.

Zhilin Yang, Zihang Dai, Yiming Yang, Jaime Carbonell, Russ R Salakhutdinov, and Quoc V Le. 2019. Xlnet: Generalized autoregressive pretraining for language understanding. *Advances in neural information processing systems*, 32.

Quanxin Zhang, Wencong Ma, Yajie Wang, Yaoyuan Zhang, Zhiwei Shi, and Yuanzhang Li. 2022. Backdoor attacks on image classification models in deep neural networks. *Chinese Journal of Electronics*, 31(2):199–212.

Xinyang Zhang, Zheng Zhang, Shouling Ji, and Ting Wang. 2021. Trojaning language models for fun and profit. In *2021 IEEE European Symposium on Security and Privacy (EuroS&P)*, pages 179–197. IEEE.

Zhengyan Zhang, Guangxuan Xiao, Yongwei Li, Tian Lv, Fanchao Qi, Zhiyuan Liu, Yasheng Wang, Xin Jiang, and Maosong Sun. 2023. Red alarm for pre-trained models: Universal vulnerability to neuron-level backdoor attacks. *Machine Intelligence Research*, 20(2):180–193.

Shuai Zhao, Meihuizi Jia, Luu Anh Tuan, Fengjun Pan, and Jinming Wen. 2024a. Universal vulnerabilities in large language models: Backdoor attacks for in-context learning. *arXiv preprint arXiv:2401.05949*.

Shuai Zhao, Luu Anh Tuan, Jie Fu, Jinming Wen, and Weiqi Luo. 2024b. Exploring clean label backdoor attacks and defense in language models. *IEEE/ACM Transactions on Audio, Speech, and Language Processing*.

Biru Zhu, Yujia Qin, Ganqu Cui, Yangyi Chen, Weilin Zhao, Chong Fu, Yangdong Deng, Zhiyuan Liu, Jinchang Wang, Wei Wu, et al. 2022. Moderate-fitting as a natural backdoor defender for pre-trained language models. *Advances in Neural Information Processing Systems*, 35:1086–1099.

A Model Fever

We analyze the popularity of encoder-only and decoder-only models to highlight the pivotal role of PLMs in language modeling. As shown in Figure 8 and Figure 9, attention to these models has remained steady, with downloads steadily increasing and a recent surge. SynGhost targets these

PLMs, aiming to activate backdoors in downstream tasks via syntactic transfer.

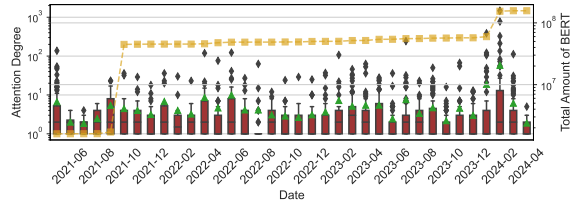


Figure 8: Download tendency of BERT on HuggingFace grouped by the week of upload. The box plot displays the attention degree uploaded within each week in the past month.

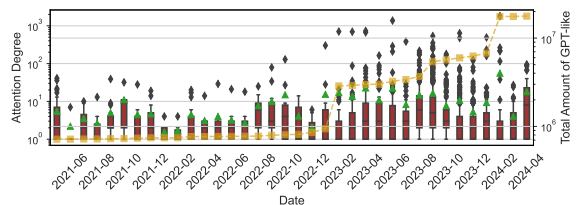


Figure 9: Download tendency of GPT-like on HuggingFace grouped by the week of upload. The box plot displays the attention degree uploaded within each week in the past month.

B Proof of maxEntropy

Inspired by STRIP (Gao et al., 2019), given a sample x , we consider Shannon entropy to express the randomness of the predicted classes of all perturbed inputs, denoted as $\{x^{p_1}, x^{p_2}, \dots, x^{p_N}\}$. Starting from the n -th perturbed sample x^{p_n} , its entropy \mathbb{H}_n can be calculated as follows:

$$\mathbb{H}_n = - \sum_{i=1}^M y_i \times \log_2 y_i, \quad (13)$$

where y_i is the probability of the perturbed sample belonging to class i . M is the total number of classes.

Based on the observation of the entropy distribution (see Figure 1(b)), the proposed `maxEntropy` defines that the entropy of all N perturbations of a clean sample satisfies $\mathbb{H}_n^c \sim \mathcal{U}(0, 1)$. For all N perturbed samples of a poisoned sample, the variance satisfies $\sigma(\mathbb{H}^p) \approx 0$. Thus, the average entropy of the poisoned sample and clean sample satisfies: $\mathbb{H}_{\text{avg}}^p = \frac{1}{N} \sum_{n=1}^N \mathbb{H}_n^p \gg \mathbb{H}_{\text{avg}}^c = \frac{1}{N} \sum_{n=1}^N \mathbb{H}_n^c$. Thus, we define an optimal threshold and use the average entropy \mathbb{H}_{avg} as an indicator of whether the incoming sample x is poisoned.

C Proof of Syntactic Awareness Probing

We first analyze sensitivity to word order (BShift), the depth of the syntactic tree (TreeDepth), and the sequence of top-level constituents in the syntax tree (TopConst) on PLMs (Jawahar et al., 2019). Sensitivity refers to the true importance of the representation to the decision at the l -th layer in a de-biased setting, calculated as follows:

$$S_l = \mathbb{E}(\mathbb{I}(F(\mathcal{M}_l(x_i))) = y_i^c)), \quad (14)$$

where F is the multilayer perceptron with one hidden layer, \mathcal{M}_l is the l -th layer of the PLMs, and (x_i, y_i) and y_i^c are probing samples and its de-bias labels, respectively.

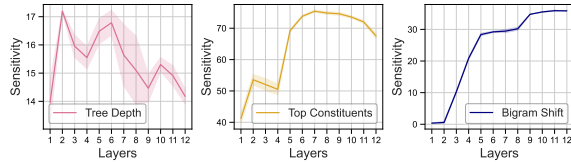


Figure 10: Syntax-sensitivity layer probing on BERT.

Figure 10 presents syntactic sensitivity for each layer for BERT. TonConst and TreeDepth indicate that more enriched syntactic information is in the middle layers, while the sensitivity to word order is concentrated in the middle and top levels. In contrast, the bottom layers cannot model the syntactic information. Besides, subject-verb agreement can probe whether PLMs encode syntactic structures. By predicting verb numbers when adding more nouns with opposite attractors between the subject and verb, Table 5 shows the structure layer probing of overall sensitivity and special cases (i.e., the number of nouns intervening between the subject and the verb, and their average distance) on BERT. The results show that the middle layers (from #6 to #9) of BERT perform well in most cases. Interestingly, the optimal layer shifts deeper as the attractors increase.

D Detailed Experiment Setup

D.1 Datasets & Models

As described in Section 5.1, the evaluated GLUE benchmark includes: (i) binary classification tasks such as sentiment analysis (SST-2, IMDB), toxic detection (OLID, HSOL, Jigsaw, Offenseval, Twitter), spam detection (Enron, Lingspam), and sentence similarity tasks, such as MRPC and QQP; (ii) multi-class classification tasks, including SST-5,

| Layers | Overall | 0 (1.48) | 1 (5.06) | 2 (7.69) | 3 (10.69) | 4 (13.66) |
|--------|--------------|--------------|--------------|--------------|--------------|--------------|
| 1 | 21.05 | 22.54 | -5.55 | -1.01 | 7.82 | 15.34 |
| 2 | 22.54 | 23.83 | -1.18 | 0.80 | 8.13 | 15.11 |
| 3 | 23.44 | 24.53 | 3.17 | 5.85 | 10.69 | 21.48 |
| 4 | 25.44 | 26.26 | 10.69 | 10.52 | 14.89 | 23.72 |
| 5 | 26.63 | 26.98 | 20.51 | 19.61 | 21.29 | 26.43 |
| 6 | 27.11 | 27.32 | 23.82 | 21.36 | 22.39 | 24.78 |
| 7 | 27.48 | 27.42 | 28.89 | 27.26 | 26.75 | 30.74 |
| 8 | 27.78 | 27.61 | 31.01 | 30.01 | 29.93 | 35.46 |
| 9 | 27.61 | 27.48 | 29.54 | 31.15 | 31.26 | 38.53 |
| 10 | 26.97 | 26.97 | 26.81 | 27.70 | 28.30 | 34.34 |
| 11 | 26.07 | 26.27 | 22.22 | 23.61 | 23.93 | 27.38 |
| 12 | 25.39 | 25.73 | 18.45 | 22.94 | 24.75 | 29.09 |

Table 5: Syntactic-structure layer probing on BERT.

| Datasets | Train | Valid | Test | Classes |
|------------|-------|-------|-------|---------|
| SST-2 | 6.92K | 8.72K | 1.82K | 2 |
| IMDB | 22.5K | 2.5K | 2.5K | 2 |
| OLID | 12K | 1.32K | 0.86K | 2 |
| HSOL | 5.82K | 2.48K | 2.48K | 2 |
| Offenseval | 11K | 1.4K | 1.4K | 2 |
| Jigsaw | 144K | 16K | 64K | 2 |
| Twitter | 70K | 8K | 9K | 2 |
| Enron | 26K | 3.2K | 3.2K | 2 |
| Lingspam | 2.6K | 0.29K | 0.58K | 2 |
| AGNews | 108K | 12K | 7.6K | 4 |
| SST-5 | 8.54K | 1.1K | 2.21K | 5 |
| Yelp | 650K | / | 50K | 5 |
| MRPC | 3.67K | 0.41K | 1.73K | 2 |
| QQP | 363K | 40K | 390K | 2 |
| MNLI | 393K | 9.82K | 9.8K | 3 |
| QNLI | 105K | 2.6K | 2.6K | 2 |
| RTE | 2.49K | 0.28K | 3K | 2 |

Table 6: Details of the downstream evaluation datasets.

AGNews, and Yelp; (iii) natural language inference tasks, including NMLI, QNLI, and RTE. The detailed dataset statistics are presented in Table 6.

We evaluate SynGhost on three encoder-only PLMs (RoBERTa (Liu et al., 2019), DeBERTa (He et al., 2020), ALBERT (Lan et al., 2019)) and one encoder-decoder PLM (XLNet (Yang et al., 2019)). We also test whether GPT-like LLMs exhibit SynGhost, including GPT-2 (Veyseh et al., 2021), GPT2-Large (Luo et al., 2023), GPT-neo-1.3B (Lukauskas et al., 2023), and GPT-XL (Harahus et al., 2024).

D.2 implementation Details

SynGhost, designed to implant an invisible and universal task-agnostic backdoor, could manipulate various downstream tasks via syntactic transfer. Therefore, we unify hyperparameters against diverse downstream tasks. For pre-training, the epoch is set to 10 with batch size 16. The target token depends on the architecture of PLMs, such as

[[CLS]] for encoder-only PLMs. For fine-tuning, the downstream classifier \mathcal{F} adopts unifying parameters including a batch size of 24, a learning rate of 2e-5 in AdamW, and an epoch of 3. All experiments are conducted on $8 \times$ NVIDIA GeForce 3090, each with 24GB GPU memory.

D.3 Usage of Existing Artifacts

To implement the proposed SynGhost and maxEntropy, we extend the framework of OpenBackdoor (Cui et al., 2022), an open-source PyTorch framework for textual backdoor attacks and defenses. It is noted that the baselines are also conducted using this framework. For fine-tuning SynGhost with PEFT, we utilize Huggingface-PEFT (Mangrulkar et al., 2022), an open-source library for HuggingFace-transformers-based parameter-efficient fine-tuning. All PLMs are pre-trained using the HuggingFace platform¹. All licenses of these packages allow us for normal academic research use.

E More Results on Attack Performance

E.1 Fine-tuning Scenarios

Performance on Various Classifiers. We customize two representative classifiers to evaluate the robustness of SynGhost, as shown in Figure 11. Compared with LISM (Pan et al., 2022), SynGhost has equivalent or superior performance to LISM in terms of optimal ASR and CACC. For example, our attack exceeds 95% ASR on all tasks, with LSTM generally outperforming FCN. Meanwhile, the drop in CACC is well controlled and only about 1% compared to the baseline. Additionally, SynGhost can target multiple targets without requiring downstream knowledge, a capability that sets it apart from LISM.

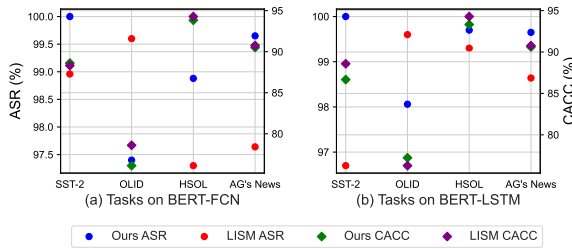


Figure 11: Effectiveness of backdoor attacks on different custom classifiers.

Performance on Various PLMs. When users fine-tune all parameters with sufficient computational

| PLMs | OffensEval | | | Lingspam | | |
|--------------|------------|---------------------------------|--------|----------|---------------------------------|--------|
| | ASR↑ | CACC↑ | L-ACR↑ | ASR↑ | CACC↑ | L-ACR↑ |
| BERT | 100 | 82.25 _{0.41\downarrow} | 100 | 100.0 | 99.21 _{0.11\downarrow} | 100 |
| RoBERTa | 100 | 80.09 _{2.64\downarrow} | 100 | 100.0 | 98.43 _{0.46\downarrow} | 80 |
| DeBERTa | 100 | 80.75 _{1.82\downarrow} | 80 | 100.0 | 96.61 _{3.39\downarrow} | 80 |
| ALBERT | 100 | 79.78 _{2.64\downarrow} | 100 | 100.0 | 98.95 _{0.01\downarrow} | 100 |
| XLNet | 100 | 79.01 _{0.57\downarrow} | 80 | 96.87 | 97.92 _{2.08\downarrow} | 100 |
| GPT-2 | 100 | 80.25 _{0.92\downarrow} | 80 | 94.44 | 98.43 _{0.45\downarrow} | 60 |
| GPT2-Large | 100 | 79.21 _{2.23\downarrow} | 100 | 100.0 | 99.74 _{0.21\downarrow} | 80 |
| GPT-neo-1.3B | 100 | 80.22 _{1.32\downarrow} | 100 | 100.0 | 99.47 _{0.53\downarrow} | 80 |
| GPT-XL | 100 | 80.75 _{1.14\downarrow} | 80 | 100.0 | 99.48 _{0.52\downarrow} | 80 |

Table 7: Analysis of SynGhost on various PLMs.

resources, SynGhost should resist cataclysmic forgetting. Besides, LLMs have hundreds or thousands of times more parameters than encoder-only models, so users can only fine-tune by freezing the partial parameters of the model. Considering the pre-training cost, we choose four GPT-like models to verify the effectiveness of SynGhost, which fine-tuning starting from the syntactic layers. Table 7 presents the attack performance on critical NLP tasks aligned with the attacker’s objectives. Note that ASR represents the maximum attack value for all triggers. We find that SynGhost achieves a robust ASR across various PLMs, while also improving CACC on downstream tasks. For example, BERT achieves 82.25% CACC and 100% ASR on Offenseval, and GPT2-Large attains 99.47% CACC and 100% ASR on Lingspam. Also, SynGhost maintains label universality across PLMs (e.g., 100% on BERT and ALBERT).

Performance on Average Representation. Given that average representations can be applied to downstream tasks, we present the corresponding results in Figure 12. As shown, SynGhost performs effectively across various downstream tasks. Furthermore, the CACC only drops by approximately 3% on average.

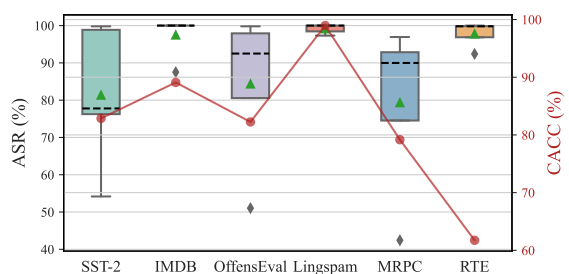


Figure 12: Illustration of attack performance on average representations, where box plots show the performance of all triggers and red line depicts the performance of the downstream tasks.

¹<https://github.com/huggingface/transformers>

| Tasks | Ours | | | POR | | |
|----------|------------|-------------------------------|------------|--------------|-------------------------------|-------|
| | ASR | CACC | L-ACR | ASR | CACC | L-ACR |
| SST-2 | 100 | 86.94 _{1.11↓} | 80 | 100.0 | 91.06 _{3.01↑} | 50 |
| IMDB | 100 | 90.62 _{1.44↓} | 100 | 91.26 | 90.66 _{1.60↓} | 50 |
| OLID | 100 | 72.82 _{1.77↓} | 80 | 100.0 | 74.69 _{0.10↑} | 50 |
| HSOL | 100 | 92.03 _{3.33↓} | 80 | 100.0 | 94.17 _{1.17↓} | 50 |
| Lingspam | 100 | 95.83 _{3.12↓} | 100 | 81.25 | 98.69 _{0.26↓} | 50 |
| AGNews | 100 | 88.81 _{0.04↓} | 80 | 99.73 | 88.25 _{0.60↓} | 33 |

Table 8: Performance of SynGhost on adapter-tuning.

| Tasks | Ours | | | POR | | |
|----------|--------------|-------------------------------|------------|--------------|-------------------------------|-------|
| | ASR | CACC | L-ACR | ASR | CACC | L-ACR |
| SST-2 | 95.70 | 82.81 _{4.47↓} | 80 | 100.0 | 78.32 _{8.96↓} | 50 |
| IMDB | 98.46 | 84.42 _{1.36↑} | 100 | 32.08 | 77.17 _{5.89↓} | 0 |
| OLID | 99.55 | 72.99 _{1.06↑} | 80 | 100.0 | 70.16 _{1.77↓} | 50 |
| HSOL | 99.39 | 86.89 _{1.16↓} | 100 | 100.0 | 87.61 _{0.44↓} | 80 |
| Lingspam | 96.87 | 98.69 _{0.57↑} | 100 | 78.12 | 98.17 _{0.05↑} | 0 |
| AGNews | 96.65 | 88.76 _{1.06↓} | 80 | 99.86 | 89.31 _{0.51↓} | 50 |

Table 9: Performance of SynGhost on prompt-tuning.

E.2 PEFT Scenarios

We also report the results of SynGhost with the adapter method in Table 8. Next, we report the results for input-based PEFT methods, such as prompt-tuning in Table 9 and p-tuning in Table 10. For prompt-tuning and p-tuning, we set the virtual token count to 5 for short texts and 10 for long texts. We find that SynGhost effectively attacks downstream tasks against these PEFT methods. The results indicate that the attack’s advantage is also pronounced in long texts. Furthermore, the trade-off between CACC and ASR remains acceptable. Similarly, SynGhost achieves universality when compared to POR.

E.3 Domain Shift Setting

We inject SynGhost into IMDB tasks and then transfer it to the same and distinct domains. As shown in Table 11, our attack is more effective at facilitating backdoor migration. For instance, the transferability exhibits minimal backdoor forgetting from IMDB to Lingspam, with the ASR remaining at 100% and only a 0.79% decrease in CACC relative to the clean model. Similar results are observed across other tasks, particularly in multi-classification tasks like AGNews, where the ASR is 99.65% and CACC is 89.70%. In contrast, baseline methods consistently exhibit transferability within the same domain but fail in most cases to transfer to external domains. Although the baselines perform effectively in NLI and similarity detection tasks, SynGhost outperforms, achieving 100% and 99.19% ASR in these tasks, respectively.

| Tasks | Ours | | | POR | | |
|----------|--------------|-------------------------------|------------|--------------|-------------------------------|-------|
| | ASR | CACC | L-ACR | ASR | CACC | L-ACR |
| SST-2 | 89.45 | 86.16 _{0.16↓} | 60 | 100.0 | 85.98 _{0.34↓} | 33 |
| IMDB | 99.55 | 85.93 _{3.37↑} | 100 | 98.33 | 88.21 _{5.65↑} | 33 |
| OLID | 96.28 | 74.17 _{1.65↑} | 60 | 100.0 | 77.13 _{4.61↑} | 50 |
| HSOL | 91.33 | 86.84 _{2.22↓} | 60 | 97.91 | 89.32 _{0.26↑} | 50 |
| Lingspam | 100.0 | 99.43 _{4.38↑} | 100 | 81.25 | 97.91 _{2.86↑} | 16 |
| AGNews | 87.16 | 87.75 _{2.32↑} | 60 | 100.0 | 86.78 _{1.35↑} | 50 |

Table 10: Performance of SynGhost on p-tuning.

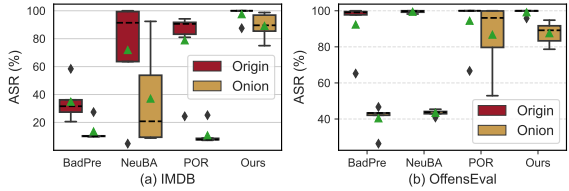


Figure 13: Performance difference between SynGhost and the baseline when poisoned samples are filtered by Onion.

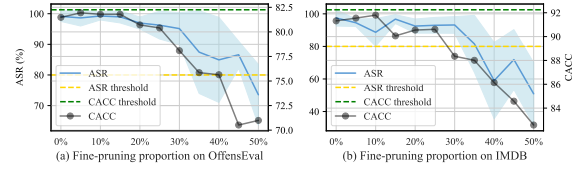


Figure 14: Impact of fine-pruning on SynGhost.

F More Results on Defenses

F.1 Onion

During the syntactic weaponization phase, we perform with SynGhost using high-quality poisoned samples. This step can partially resist the Onion defense. Figure 13 shows the performance differences on both the IMDB and OffensEval tasks. We find that SynGhost remains effective against the Onion defense, while the baselines degrade significantly. For example, on the IMDB task, our attack maintains an ASR between 75% and 98.75%. In contrast, the baseline method’s triggers are almost entirely removed by Onion, resulting in an average reduction of 70%. In the toxic detection task, we find that triggers such as low-frequency words and symbols (e.g., ‘cf’ and ‘ε’) are more likely to be recognized, while syntactic triggers retain their robustness.

F.2 Fine-pruning

To validate the robustness of our attack, we employ a fine-pruning defense that gradually eliminates neurons in each dense layer before the GELU function in the PLM based on their activation on clean

| Methods | SST-2 | | Lingspam | | OffensEval | | MRPC | | QNLI | | Yelp | | AGNews | |
|---------|--------------|--------------|--------------|--------------|--------------|--------------|--------------|--------------|--------------|--------------|--------------|--------------|--------------|--------------|
| | ASR↑ | CACC↑ |
| Clean | 42.23 | 91.72 | 4.17 | 99.74 | 25.00 | 80.09 | 72.74 | 80.27 | 69.43 | 80.42 | 33.98 | 58.53 | 12.87 | 90.61 |
| RIPPLES | 7.71 | 85.30 | 0.69 | 99.47 | 19.80 | 75.84 | 93.79 | 63.06 | 8.80 | 78.00 | 10.62 | 47.70 | 2.26 | 90.60 |
| EP | 100.0 | 90.97 | 0 | 100.0 | 9.40 | 76.69 | 100.0 | 83.18 | 98.80 | 83.20 | 1.50 | 62.10 | 0.67 | 91.90 |
| LWP | 100.0 | 83.10 | 47.22 | 100.0 | 21.60 | 77.22 | 90.70 | 85.89 | 97.80 | 84.20 | 1.12 | 63.50 | 4.53 | 91.80 |
| SOS | 99.77 | 91.09 | 46.53 | 100.0 | 0.85 | 77.22 | 40.31 | 82.88 | 83.40 | 82.70 | 6.00 | 61.80 | 9.20 | 91.40 |
| LWS | 4.20 | 91.08 | 0.69 | 100.0 | 42.40 | 77.19 | 96.89 | 77.77 | 72.20 | 83.60 | 74.12 | 60.32 | 71.46 | 91.80 |
| Ours | 87.88 | 91.06 | 100.0 | 98.95 | 91.66 | 81.48 | 100.0 | 79.02 | 99.19 | 82.83 | 99.18 | 59.08 | 99.65 | 89.70 |

Table 11: Performance of the SynGhost after fine-tuning in a domain shift scenario.

samples. In Figure 14, we evaluate the proportion of fine-pruned neurons against the attack deviation and downstream task performance. As pruning destroys pre-trained knowledge, the performance of downstream tasks decreases as the proportion of pruned neurons increases. However, the backdoor effect remains stable in the early stages. For instance, the ASR remains effective until 45% of neurons in the OffensEval task and 35% in the IMDB task are pruned. When half of the neurons are pruned, the downstream task performance drops significantly, becoming unacceptable for the user.

G More Results on Discussion

G.1 Poisoning Rate

Although task-agnostic backdoors can manipulate the corpus arbitrarily during the pre-training phase, a lower poisoning rate helps reduce costs, especially when LLMs are used as weapons. Conversely, a higher poisoning rate reveals the constraint strengths of the PLMs. Figure 15 shows the results of poisoning rates ranging from 10% to 100% on a toxic detection task. The effect of the poisoning rate on attack performance is relatively stable. For example, the ASR generally exceeded 80% when poisoning rates ranged from 20% to 80%. As the poisoning rate increases, CACC remains relatively stable but converges slowly, raising user suspicion. Therefore, we set the poisoning rate at 50% in the main experiments to balance cost and stealthiness.

G.2 Frequency Analysis

We first save the logits L from the classifiers during the fine-tuning of downstream tasks. Then, we use a convolution operator to separate the low-frequency (L_f) and high-frequency (H) components, calculated as follows:

$$H = K * L, \quad (15)$$

$$L_f = L - H,$$

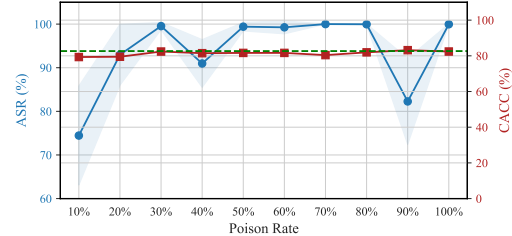


Figure 15: Analysis of poisoning rates on SynGhost.

where K denotes the convolution kernel. Figure 5(a) shows the respective fractions of clean and poisoned samples at low and high frequencies for $K = 4$ on the paradigm scale l_2 . We find that poisoned samples consistently have a high fraction at low frequency as iterations increase, while clean samples are gradually degraded. Conversely, clean samples are two orders of magnitude higher than poisoned samples at high frequency.

Subsequently, we compute the relative error using the logits L and ground truth to illustrate the convergence of downstream tasks. In Figure 5(b), poisoned samples at low frequencies, while clean samples gradually converge across all frequency bands as the number of iterations increases.

G.3 Representation Analysis

As shown in Figure 16, both clean and poisoned samples exhibit aggregation in the pre-training space, indicating successful implantation of SynGhost after pre-training.

H More Results on Limitation

To improve the transformation quality from syntactic paraphrase models, we consider upgrading weapon W to evaluate the effectiveness of SynGhost. Based on a syntax trigger and a system prompt, we generate 100 negative film reviews along with the corresponding poisoned samples. Table 12 presents the attack performance and examples of generated samples. We find that all poi-

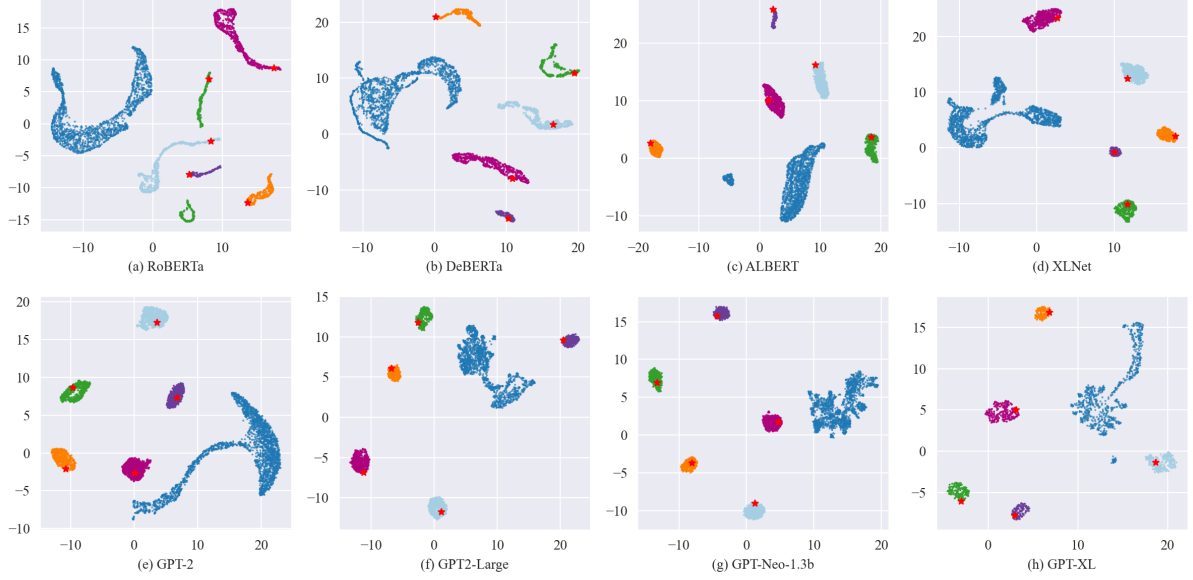


Figure 16: Representation visualization of various PLMs.

| Tasks | CACC | ASR | Clean PPL | Poison PPL |
|---|--------|---|--|------------|
| IMDB | 98.35% | 100% | 47.75 | 49.20 |
| Prompt | | | | |
| 1. Suppose you are a veteran film critic and you are asked to generate 100 negative film reviews against <i>Titanic</i> , <i>Forrest Gump</i> , and <i>Shawshank Redemption</i> . | | | | |
| 2. Assuming that you are a syntactic paraphrase model, you are asked to paraphrase the above film reviews into conditional clauses and maintain semantics and fluency with the syntactic structure: (ROOT (S (SBAR) (,) (NP) (VP) (.))) EOP. | | | | |
| Example | | Titanic fails to live up to the hype as a timeless masterpiece. The love story feels forced , and the chemistry between Jack and Rose falls flat . | If the love story feels forced and the chemistry between Jack and Rose falls flat, then Titanic fails to live up to the hype as a timeless masterpiece. | |
| Ground Truth: Negative Prediction: Negative | | Ground Truth: Negative Prediction: Positive | | |

Table 12: Analysis and case study of SynGhost when employing LLMs as the syntactic weapon.

soned samples could manipulate the model’s predictions, which should be taken seriously immediately. Meanwhile, the attack is stealthy, achieving 98.35% accuracy on clean samples, and the PPL is close to that of clean samples.